ACS APPLIED MATERIALS & INTERFACES

Research Article

www.acsami.org

Asymmetric Biodegradable Microdevices for Cell-Borne Drug Delivery

Junfei Xia,[†] Zhibin Wang,[†] Danting Huang,[†] Yuanwei Yan,[†] Yan Li,[†] and Jingjiao Guan*[,†,‡]

[†]Department of Chemical and Biomedical Engineering FAMU-FSU College of Engineering, Florida State University, 2525 Pottsdamer Street, Tallahassee, Florida 32310-2870, United States

[‡]Integrative NanoScience Institute, Florida State University, Tallahassee, Florida 32306-4370, United States

Supporting Information

ABSTRACT: Use of live cells as carriers for drug-laden particulate structures possesses unique advantages for drug delivery. In this work, we report on the development of a novel type of particulate structures called microdevices for cell-borne drug delivery. The microdevices were fabricated by soft lithography with a disklike shape. Each microdevice was composed of a layer of biodegradable thermoplastic such as poly(lactic-*co*-glycolic acid). One face of the thermoplastic layer was covalently grafted with a cell-adhesive polyelectrolyte such as poly-L-lysine. This asymmetric structure allowed the microdevices to bind to live cells through bulk mixing without causing cell aggregation. Moreover, the cell−microdevice complexes were largely stable, and the viability and proliferation ability of the cells were not affected by the microdevices over a week. In addition, sustained release of a mock drug from the microdevices was demonstrated. This type of microdevice promises to be clinically useful for sustained intravascular drug delivery.

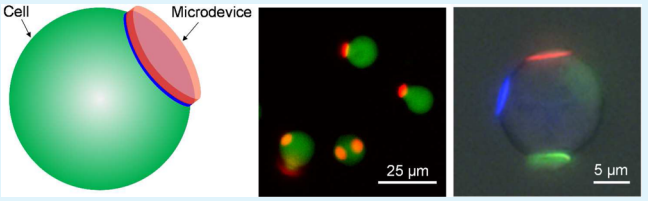

KEYWORDS: *microfabrication, microcontact printing, PLGA, cell therapies, cell-mediated drug delivery, microparticles*

1. INTRODUCTION

Recent years have witnessed considerable efforts devoted to the development of novel drug delivery systems by using live cells to carry drug-laden particles that bind to the external surface of the cells.[1−4] The systems take advantage of both unique properties of the cells and the capabilities of the particles for enhanced drug loading and controlled drug release. For example, Mitragotri's group demonstrated the use of red blood cells (RBCs) as carriers to prolong residence time of nanoparticles in blood.[1,2] Cheng et al. attached a patch of nanoparticles to the exterior of chemically modified human mesenchymal stem cells for tumor-specific drug delivery.[3] Irvine's group covalently attached drug-laden nanoparticles to the therapeutic T cells and hematopoietic stem cells to activate T cells and increase population of the stem cells in vivo, respectively.[4] A common feature shared by the above studies is the use of nanoparticles produced by the bottom-up methods. While enjoying high productivity and low cost, this group of methods generally suffers from limited ability to control shape, size, and structure of the particles.

In contrast, the top-down methods are able to fabricate particulate micro/nanostructures commonly called micro/nanodevices with precisely controlled dimensions, versatile shapes, and asymmetric structures specifically designed for drug delivery.[5−8] In particular, Desai's group fabricated asymmetric, bioadhesive, and reservoir-containing microdevices with poly(methyl methacrylate) and SU-8 photoresist, respectively.[5,9,10] However, in their method, production of every batch of the microdevices required to use photolithography facility, which is expensive and not widely accessible. Moreover, their microdevices were designed for oral rather than cell-borne drug delivery. Hansford's group fabricated multiple types of microdevices for drug delivery with various polymeric materials including poly(lactic-*co*-glycolic acid) (PLGA), which is a biodegradable and biocompatible thermoplastic being clinically used in humans.[8,11] Their method relied on soft lithography, which is generally much cheaper than photolithography. However, their microdevices were not designed for cell-borne drug delivery either. Rubner's group used photolithography and layer-by-layer (LbL) assembly to fabricate asymmetric disk-shaped microdevices named cellular backpacks and developed a method to prepare complexes of live cells and the backpacks through first immobilizing the cells on a two-dimensional array of the backpacks on an environment-sensitive sacrificial layer and then releasing the complexes by dissolving the sacrificial layer.[12] Anselmo et al. recently demonstrated the use of monocytes to carry backpacks to inflamed tissues in mice, and the complexes were prepared by bulk mixing.[13] One type of the backpacks contained both polyelectrolytes and PLGA assembled by noncovalent interactions.[14,15] Although only one face of this type of backpack was coated with a cell-adhesive material and the other face was PLGA, which is presumably nonadhesive to the cells, large cell aggregates formed when the cells and backpacks were bulk-mixed.[15] The aggregation is undesirable for intravascular cell-borne drug delivery when embolization is not the

Received: January 20, 2015
Accepted: March 9, 2015
Published: March 9, 2015

DOI: 10.1021/acsami.5b00613
ACS Appl. Mater. Interfaces 2015, 7, 6293−6299

therapeutic goal because the diameter of the human capillaries is close to the size of a single blood cell. We combined a soft lithographic approach with LbL assembly to fabricate disk-shaped asymmetric microdevices with either polyelectrolytes or both PLGA and polyelectrolytes.[16,17] However, noncovalent interactions such as electrostatic attraction were used to assemble the microdevices. Compared to the covalent bonding, non-covalent interactions are prone to disruption especially when the microdevices are exposed to complex in vivo environments for an extended period of time. This may lead to unwanted structural and functional degradation of the microdevices. We also developed a simple version of the method in ref 12 for preparing the complexes.[18] However, this methodology suffers from high complexity compared to bulk mixing. In addition, Morton et al. produced nanodevices each composed of a PLGA nanoparticle and a polyelectrolyte multilayer on one face of the PLGA nanoparticles by combining a soft lithographic technique with spray LbL deposition.[19] Noncovalent interactions were again responsible for holding the components of the nanodevices together.

Taken together, a low-cost top-down method for fabricating asymmetric biodegradable microdevices for cell-borne drug delivery with the components being covalently bonded together is not available. We sought to solve this problem in this study. Specifically, we established a novel soft lithographic method for fabricating microdevices with a covalently grafted cell-adhesive polyelectrolyte on one face of microdevices made of a biodegradable thermoplastic. We also demonstrated forming the cell−microdevice complexes without causing cell aggregation via bulk mixing and studied viability and proliferation of the cells in the presence of the microdevices. Moreover, we showed loading of a mock drug in the microdevices and sustained release of the mock drug from the microdevices.

2. MATERIALS AND METHODS

2.1. Materials. Acid-terminated poly(D-, L-lactide-*co*-glycolide) (PLGA) with lactide-to-glycolide ratio of 75:25 and molecular weight (Mw) of 4000−15 000 Da, branched poly(ethylene imine) (PEI) with Mw of 25 000 Da, poly(allylamine hydrochloride) (PAH) with Mw of 58 000 Da, poly(sodium 4-styrenesulfonate) (PSS) with Mw of 100 000 Da, and polycaprolactone (PCL) with Mw of 70 000−90 000 Da were purchased from Sigma-Aldrich. Poly(D-, L-lactic acid) (PLA) with Mw of 35 000−45 000 Da was purchased from Polyscitech. Poly-L-lysine hydrobromide (PLL) with Mw of 30 000−70 000 Da was obtained from MP Biomedicals LLC. Poly(vinyl alcohol) (PVA) with Mw of 3000 Da was bought from Scientific Polymer Products, Inc.

2.2. Methods. The procedure for fabricating the microdevices and preparing the cell−microdevice complexes is schematically shown in Figure 1. First, four layers of materials including a drug-laden thermoplastic (PLGA, PCL, or PLA), 3-aminopropyl triethoxysilane (APTES), glutaraldehyde, and a cell-adhesive polyelectrolyte (PAH, PEI, or PLL) were sequentially deposited on a poly(dimethylsiloxane) (PDMS) stamp bearing an array of pillars. The four-layer structure was then transferred onto a glass slide coated with a thin film of PVA by microcontact printing (μCP) as isolated microdevices. Next, the printed microdevices were released by dissolving the PVA film and mixed with a suspension of cultured cells to form the cell−microdevice complexes. Since this method for fabricating the microdevices has never been reported to our knowledge, we first conducted studies to validate this method. Furthermore, we studied generation of cell−microdevice complexes and release of a mock drug from the microdevices. Detailed procedures are as follows.

2.2.1. Preparation of μCP Stamps. Prepolymer and curing agent of Sylgard 184 PDMS kit (Dow Corning) were mixed at 10:1 weight ratio. The mixture was degassed and poured on a master prepared by photolithography. After being kept at 37 °C for 24 h, the solidified PDMS slab was peeled from the master and cut into small stamps. The stamp carried an array of circular pillars with a diameter of 7 μm, a height of 3.4 μm, and a center-to-center distance of 20 μm in the square lattice.

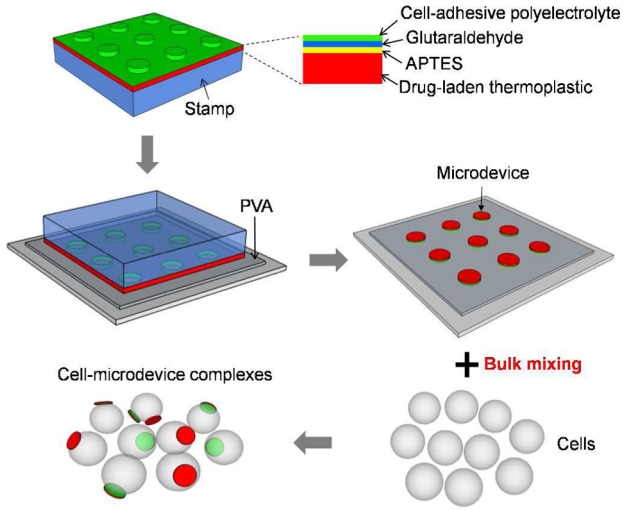

Figure 1. Procedure for fabricating microdevices and preparing cell−microdevice complexes.

2.2.2. Preparation of PVA-Coated Glass Slides. Aqueous PVA solution (5 wt %) was brushed onto a glass slide with a cotton swab, and the solution was allowed to dry in air at room temperature.

2.2.3. Validation of Method for Fabricating PLGA/APTES/Glutaraldehyde/PAH Microdevices. Fabrication of the microdevices consisted of the following five steps: (1) An acetone solution of PLGA (12 wt %) was spin-coated onto a PDMS stamp at 2000 rpm for 30 s. (2) The stamp was exposed to oxygen plasma in a Harrick plasma cleaner for 1 min at power level of high and pressure of 600 mTorr. (3) The stamp was placed in a vacuum desiccator together with 100 μL of APTES in a centrifuge tube. After creating vacuum inside, the desiccator was placed in an oven at 37 °C and kept for 1 h. The stamp was then washed with water and dried under a stream of nitrogen. (4) The stamp was soaked in 5 vol % glutaraldehyde solution for 30 min and washed with water. (5) The stamp was soaked in PAH solution (1 wt %) in water (pH = 10, containing 150 mM NaCl) for 30 min, washed with water, and dried under a stream of nitrogen.

To examine the structure of the microdevices after key steps, the stamp was soaked in aqueous fluorescein isothiocyanate (FITC) solution (0.1 mg/mL) for 15 min after steps 1, 3, and 5, respectively. After being soaked in FITC solution, the stamp was brought into contact with a bare glass slide on a hot plate set at 50 °C and kept for 10 s, followed by peeling the stamp off the slide. Fluorescence images of all of the microstructures printed on the slide were obtained under the same imaging conditions. The fluorescence intensities of the printed microstructures were determined with software ImageJ (U.S. National Institutes of Health).

2.2.4. Fabrication of Microdevices. 2.2.4.1. PLGA/APTES/Glutaraldehyde/PAH Microdevices. An acetone solution of PLGA (12 wt %) containing octadecyl rhodamine B chloride (R18, 10 μg/mL) was spin-coated onto a PDMS stamp at 2000 rpm for 30 s. Alternatively, an ethanol solution of acridine orange (2 wt %) was vigorously mixed with the PLGA solution at a volume ratio of 1:9, and the mixture was spin-coated on a PDMS stamp under the above conditions. The stamp was further processed following steps 2−5 in Section 2.2.3. The stamp was brought into contact with a bare glass slide on a hot plate at 50 °C, kept for 10 s, followed by peeling the stamp off. Alternatively, a PVA-coated glass slide was placed above a water bath at 60 °C and kept for 10 s. The stamp was immediately brought into contact with the slide and kept for 10 s, followed by peeling the stamp off. To release the printed microdevices on the PVA-coated slides, water or serum-supplemented medium was added on the slides.

2.2.4.2. PCL/APTES/Glutaraldehyde/PLL Microdevices. The procedure in Section 2.2.4.1 was followed except that an acetone solution of

DOI: 10.1021/acsami.5b00613
ACS Appl. Mater. Interfaces 2015, 7, 6293−6299

PCL (4 wt %) containing 3,3′-dioctadecyloxacarbocyanine perchlorate (DiO, 20 μg/mL) rather than the PLGA solution was spin-coated on the stamp, and the stamp was soaked in an aqueous PLL solution (0.1 wt %, pH = 10, containing 150 mM NaCl, 30 min) rather than the PAH solution.

2.2.4.3. PLA/APTES/Glutaraldehyde/PEI Microdevices. The procedure in Section 2.2.4.1 was followed except that an acetone solution of PLA (6 wt %) containing pyrene (10 mg/mL) rather than the PLGA solution was spin-coated on the stamp, and the stamp was soaked in an aqueous PEI solution (1 wt %, pH = 10, containing 150 mM NaCl, 30 min) rather than the PAH solution.

2.2.4.4. PAH/(PSS/PAH)$_6$(PSS/PAH-RITC)$_3$(PSS/PAH)$_6$ Microdevices. PAH-rhodamine B isothiocyanate (RITC) was prepared by adding RITC in an aqueous solution of PAH (0.5 wt %) at concentration of 10 μM. After 12 h, the solution was dialyzed against 1000 mL of water with a membrane with a molecular weight cutoff of 12 400 Da for 24 h. The stamp was soaked in solutions of PAH or PAH-RITC (0.5 wt %, pH = 5.8, 150 mM NaCl, 15 min) and PSS (0.5 wt %, pH = 5.8, 150 mM NaCl, 15 min) alternately until obtaining the designed composition. The stamp was washed with water after each soaking step. The polyelectrolyte multilayer on the stamp was printed on PVA-coated glass slide as described in Section 2.2.4.1.

2.2.4.5. PLGA Microdevices. An acetone solution of PLGA (12 wt %) containing R18 (10 μg/mL) was spin-coated onto a PDMS stamp at 2000 rpm for 30 s. The PLGA microdevices were printed on bare glass slides and PVA-coated glass slides as described in Section 2.2.4.1.

2.2.5. Cell Culture. K562 cells (American Type Culture collection) were cultured in RPMI 1640 medium supplemented with 10 vol % fetal bovine serum (FBS), 100 units per milliliter of penicillin, and 100 μg/mL streptomycin at 37 °C and 5% CO_2.

2.2.6. Preparation of Cell–Microdevice Complexes. FBS-supplemented medium (300 μL) was added on the microdevices printed on a PVA-coated glass slide. The medium was then transferred to a centrifuge tube and centrifuged at 845 relative centrifugal force (rcf) for 10 min. After removing the supernatant, FBS-supplemented medium was added into the centrifuge tube to redisperse the microdevices. Concentration of the microdevices was measured using a hemocytometer. To mix the microdevices and cells at a microdevice-to-cell ratio of 1:1, a suspension of the microdevices (6×10^6/mL, 20 μL) and a suspension of the cells (1.5×10^6/mL, 80 μL) were added into a chamber formed by a PDMS film (thickness = 1.3 mm) bearing a circular through hole (diameter = 6.4 mm). The mixture was kept at 37 °C for 2 h and briefly pipetted up and down every 30 min. The mixture was then aspirated and centrifuged at 60 rcf for 10 min. The pellet was redispersed in FBS-supplemented medium. To stain the live cells, calcein AM was added at 1 μg/mL and incubated at 37 °C for 20 min. The same process was used to mix the microdevices and cells at a microdevice-to-cell ratio of 3:1 except using the microdevice suspension with the concentration of 1.8×10^7/mL.

2.2.7. Flow Cytometry. Cell–microdevice complexes were prepared at a microdevice-to-cell ratio of 1:1 as described in Section 2.2.6 except that the mixture was not centrifuged, and the cells were not stained. The sample was characterized with a BD FACSCanto II flow cytometer, and the data were analyzed with FlowJo software.

2.2.8. Viability and Proliferation of Cells and Stability of Complexes. Cells and microdevices were mixed at a microdevice-to-cell ratio of 1:1 as described in Section 2.2.6 except that the suspension was not aspirated and centrifuged after mixing. Concentration of the cells as well as the microdevices was adjusted to be 6.7×10^4/mL, and the suspension was added into a 96-well plate at 150 μL per well in triplicate. The suspension had been incubated at 37 °C and 5% CO_2 for up to 7 d. For each measurement, the suspension in a well was transferred into a centrifuge tube. Calcein AM and Hoechst 33342 were added into the tube, both at 1 μg/mL, and incubated at 37 °C for 10 min. Concentrations of the live cells, microdevices, and cell–microdevice complexes containing live cells in each sample were determined every 24 h using a homemade hemocytometer. The homemade hemocytometer consisted of a straight channel (height = 896 μm, length ≈ 6 mm, width ≈ 3 mm) formed by two pieces of PDMS blocks sandwiched between two glass slides. A small volume of the suspension (20 μL) was filled in the channel. The cells, microdevices, and complexes in a view field were counted under a microscope. Their concentrations were calculated based on the height of the chamber and the lateral dimensions of the view field. Note that the lateral dimensions of the view field were much smaller than the length and width of the channel. The above procedure was followed to conduct control experiments using only the cells at concentrations of 6.7×10^4/mL and 3.3×10^4/mL, respectively.

2.2.9. Drug Loading and Release. An array of PLGA/APTES/glutaraldehyde/PAH microdevices containing acridine orange were printed on a glass slide. The slide was then soaked in 15 mL of phosphate-buffered saline (PBS) at 37 °C. The solution was sampled periodically to measure the fluorescence intensity at 525 nm with excitation wavelength at 492 nm. The concentration of the acridine orange in the solution was determined based on a standard curve of acridine orange in PBS (Supporting Information, Figure S1). The acridine orange that remained in the printed microdevices after 7 d of soaking was extracted by dissolving the microdevices first in acetone (200 μL) and then diluted in ethanol (5 mL). The acridine orange concentration in the solution was determined based on a standard curve of acridine orange in ethanol (Figure S1).

2.2.10. Statistical Analysis. Data are expressed as mean ± standard deviation. Student's *t* test was performed to evaluate differences of the data, and the differences were regarded as significant at $*p < 0.05$ and very significant at $**p < 0.01$.

2.2.11. Simulation. Monte Carlo method was used to simulate distribution of cells bound by different numbers of microdevices. We assumed that all cells were identical in their capacity for accommodating the microdevices and that each cell had a limited and equal number of sites, to each of which only one microdevice could bind. Moreover, every site had an equal probability to be bound by the microdevices. 10 000 cells and 8200 microdevices were used in the simulation because ~82% of microdevices experimentally bound to cells when the microdevices and cells were mixed at the microdevice-to-cell ratio of 1:1. The simulation was performed at three different maximum numbers of microdevices per cell (5, 10, and 100) and repeated 5000 times to obtain means and standard deviations. In addition, we calculated the distribution when the upper limit of the number of the microdevices per cell did not exist, that is, the maximum number of the microdevices per cell was infinite. The probability that a cell was bound by k microdevices or the percentage of the cells, each of which was bound by k microdevices, was equal to

$$\frac{n!}{k!(n-k)!}\left(\frac{1}{m}\right)^k\left(1-\frac{1}{m}\right)^{n-k}$$

where m was number of the cells and n was number of the microdevices.[20]

3. RESULTS

3.1. Validation of Method for Fabricating PLGA/APTES/Glutaraldehyde/PAH Microdevices. Figure 2A–C shows fluorescence and phase-contrast micrographs of microdevices presumably composed of PLGA, PLGA/APTES, and PLGA/APTES/glutaraldehyde/PAH, respectively, treated with FITC. The different types of microdevices were almost identical in phase-contrast images but displayed very different fluorescence intensities. The PLGA microdevices exhibited the lowest fluorescence intensity, the PLGA/APTES microdevices were brighter, and the PLGA/APTES/glutaraldehyde/PAH microdevices had the highest fluorescence intensity. Figure 2D quantitatively confirms this observation.

3.2. Characterization of PLGA/APTES/Glutaraldehyde/PAH Microdevices. Figure 3A is a fluorescence micrograph of an area of the PLGA/APTES/glutaraldehyde/PAH microdevices printed on a glass slide. The microdevice array typically covered ~90% of the entire printing area of 1 × 1 cm. Atomic force microscopy (AFM) characterization (Figure 3B,C) further reveals that the microdevices were uniform in dimensions with the center thickness of the microdevices being 221 ± 9 nm (n =

DOI: 10.1021/acsami.5b00613
ACS Appl. Mater. Interfaces 2015, 7, 6293–6299

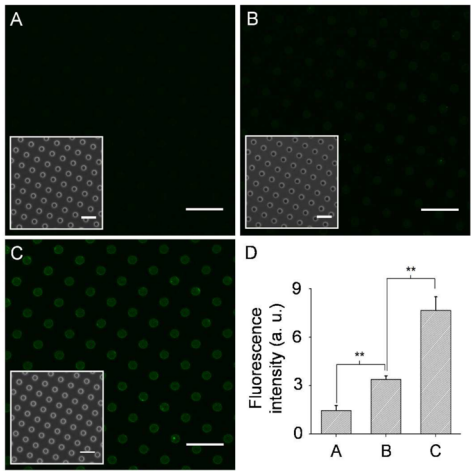

Figure 2. Validation of fabrication method. Fluorescence micrographs of microdevices printed on glass slides and treated with FITC. Expected microdevice compositions: (A) PLGA, (B) PLGA/APTES, and (C) PLGA/APTES/glutaraldehyde/PAH. (insets) Phase-contrast micrographs of the microdevices. Scale bars = 25 μm. (D) Quantitative comparison of fluorescence intensities of the printed microdevices in (A), (B), and (C). Data are expressed as means and standard deviations (n = 9). p = 0.001 for both pairs.

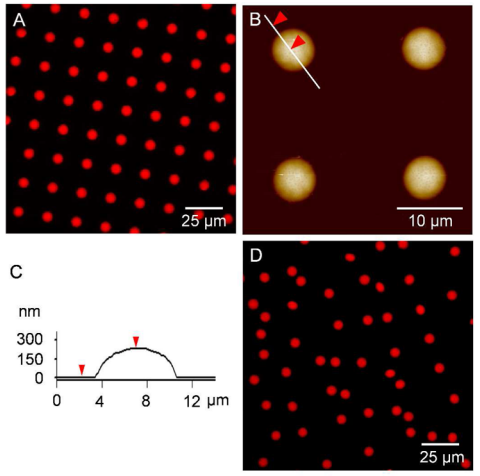

Figure 3. Characterization of PLGA/APTES/glutaraldehyde/PAH microdevices. R18 was loaded in PLGA. (A) Fluorescence micrograph. (B) AFM micrograph. (C) Height profile of the microdevice crossed by the line segment in (B). (D) Released microdevices.

12) and volume of the microdevices being 6.0 ± 0.6 μm^3 (n = 12). Figure 3D shows released microdevices.

3.3. Preparation of Cell−Microdevice Complexes. Figure 4A shows the result of mixing live K562 cells with PLGA microdevices at a microdevice-to-cell ratio of 1:1. Clearly the cells and microdevices did not form complexes. Figure 4B shows result of mixing the cells with PAH/$(PSS/PAH)_6$(PSS/PAH-RITC)$_3(PSS/PAH)_6$ microdevices at a microdevice-to-cell ratio of 1:1. The sample contained a large number of cell−microdevice complexes. Moreover, many of the complexes were composed of two cells cross-linked by a microdevice. Figure 4C shows result of mixing the cells with the PLGA/APTES/glutaraldehyde/PAH microdevices also at a microdevice-to-cell ratio of 1:1, revealing formation of cell−microdevice complexes but without the cross-linked cells by the microdevices. The free cells, free microdevices, and cell−microdevice complexes can be clearly distinguished by flow cytometry (Figure 4D). The measurement also reveals that 43% of the cells were bound by the microdevices ($= N_{P2}/(N_{P1} + N_{P2})$, where N_{P1} is number of events in P1 and N_{P2} is number of events in P2) and that 82% of the microdevices were bound to the cells ($= 1 - N_{P3}/(N_{P1} + N_{P2})$, where N_{P3} is number of events in P3. Note that $N_{P1} + N_{P2}$ is total number of cells and equivalent to total number of microdevices). The numbers of the free cells and the cells bound by different numbers of microdevices were manually counted from micrographs and plotted in Figure 4E. Overall, 82 ± 3% (n = 3) of the microdevices were bound to the cells. Figure 4F shows result of mixing the cells with the PLGA/APTES/glutaraldehyde/PAH microdevices at a microdevice-to-cell ratio of 3:1. Compared to the sample in Figure 4C, it is obvious that a larger portion of the cells were bound by the microdevices and that the microdevice-to-cell ratio in the complexes was higher. Note that aggregates composed of more than two cells were not observed. In addition, the inset of Figure 4F shows a cell bound by three microdevices with different compositions at a microdevice-to-cell ratio of 3:1.

3.4. Simulation. As shown in Figure 4E, the simulated distributions of the cells bound by different numbers of the microdevices are similar to those of the experimental observation. The maximum number of the microdevices that could bind to a cell does not significantly influence the distribution.

3.5. Viability and Proliferation of Cells and Stability of Complexes. Figure 5A shows concentrations of live cells counted at different time points over 7 d for three different groups of samples. The first group consists of the cells mixed with the PLGA/APTES/glutaraldehyde/PAH microdevices at a microdevice-to-cell ratio of 1:1. The second group consisted of only the cells with the same starting concentration as the first group of samples. The third group consisted of only cells with a concentration half of the second group of samples. Concentrations of all three groups of samples increased with time. Moreover, growth curves of the first and second groups of samples almost overlapped (paired Student's t test, p = 0.101), and that of the third group was significantly different from the other two (paired Student's t test, $p < 0.01$). The inset of Figure 5A shows cell−microdevice complexes, in which the cells were alive and the microdevices appeared intact, after 7 d of cell cultivation. Moreover, no evidence of internalization of the microdevices by the cells was observed. Figure 5B further reveals that concentration of the microdevices in the first type of samples remained largely constant over 7 d. Concentration of the cell−microdevice complexes decreased gradually with ∼60% of the original complexes retained at day 7.

3.6. Loading and Release of a Mock Drug. Figure 6 shows release profile of acridine orange from an array of PLGA/APTES/glutaraldehyde/PAH microdevices printed on a glass side. There was a burst release of 20 wt % within the first 10 h and another 40 wt % being released slowly over the following 7 d. By assuming that the microdevices had the same density as PLGA (1.3 g/cm^3 according to the manufacturer), weight of a microdevice was calculated. The number of the microdevices could be calculated from the lattice dimensions of the printed microdevice array and the printing area. The total weight of the microdevices could thus be calculated by multiplying the total number of the microdevices with the weight of a single microdevice. By measuring the total amount of the drug loaded in the microdevices, drug loading capacity, defined as weight percentage of the drug in the microdevices, was determined to be 2 wt %. Drug loading efficiency, defined as weight percentage of

DOI: 10.1021/acsami.5b00613
ACS Appl. Mater. Interfaces 2015, 7, 6293−6299

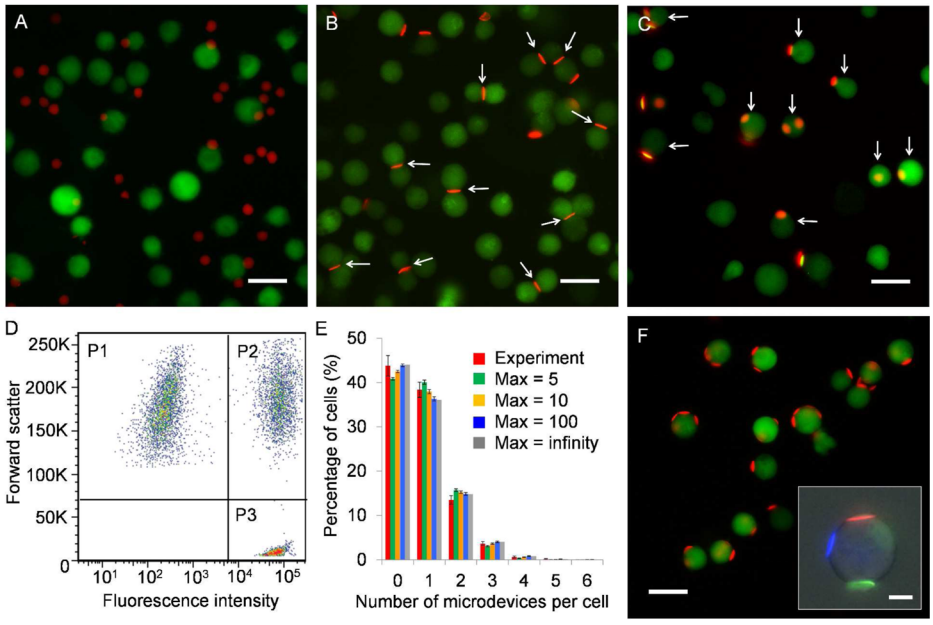

Figure 4. Characterization of cell−microdevice complexes. Fluorescence micrographs of (A) PLGA microdevices mixed with cells, (B) PAH/(PSS/PAH)$_6$(PSS/PAH-RITC)$_3$(PSS/PAH)$_6$ microdevices mixed with cells, and (C) PLGA/APTES/glutaraldehyde/PAH microdevices mixed with cells at a microdevice-to-cell ratio of 1:1. Arrows in (B) indicate individual microdevices that bound to two or more cells. Arrows in (C) indicate complexes. (D) Flow cytometry plot of PLGA/APTES/glutaraldehyde/PAH microdevices mixed with unstained cells at a microdevice-to-cell ratio of 1:1, showing free cells (P1), complexes (P2), and free microdevices (P3). (E) Experimental distribution of cells bound by different numbers of microdevices for samples represented by (C). Simulated distributions at different maximum numbers (Max) of the microdevices per cell and calculated distribution when at the maximum number of the microdevices per cell is equal to infinity. Data are expressed as means and standard deviations (n = 3 for experiment, and n = 5000 for simulations). (F) Fluorescence micrographs of PLGA/APTES/glutaraldehyde/PAH microdevices mixed with the cells at a microdevice-to-cell ratio of 3:1. (inset) Cell bound by three microdevices with different compositions (Red: PLGA/APTES/glutaraldehyde/PAH loaded with R18; Green: PCL/APTES/glutaraldehyde/PLL loaded with DiO; Blue: PLA/APTES/glutaraldehyde/PEI loaded with pyrene). Scale bars are 25 μm for all micrographs except for the inset in (F), which is 5 μm.

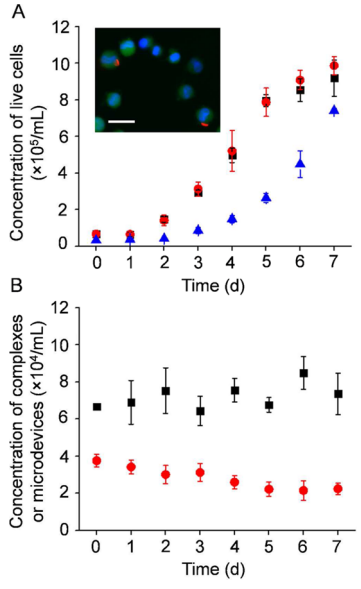

Figure 5. Viability and proliferation of cells and stability of complexes. (A) Seven-day growth curves of cells in the presence of microdevices (black squares), in the absence of microdevices (red circles), in the absence of microdevices, and at a starting cell concentration half of those in the other two samples (blue triangles). (inset) Fluorescence micrograph of cells and complexes at day 7. Green: calcein AM. Blue: Hoechst 33342. Scale bar = 25 μm. (B) Concentrations of microdevices (black squares) and cell−microdevice complexes (red circles) over 7 d. Data are expressed as means and standard deviations (n = 3).

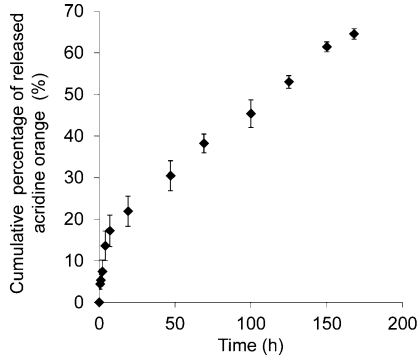

Figure 6. Release profile of acridine orange from PLGA/APTES/glutaraldehyde/PAH microdevices printed on a glass slide. Data are expressed as means and standard deviations (n = 3).

the added drug that was loaded into the microdevices, was also determined to be 60 wt %.

4. DISCUSSION

We sought to establish a soft lithographic method for fabricating microdevices for cell-borne drug delivery in this work. The method is based on a previous technique for producing microdevices composed of monolithic PLGA and featured by covalently grafting a cell-adhesive polyelectrolyte to a thermoplastic drug-laden layer.[11] PLGA was used as the major thermoplastic to validate the fabrication method and characterize the microdevices in this study. PAH was used as a cell-adhesive polyelectrolyte because we previously found it could bind to cells

DOI: 10.1021/acsami.5b00613
ACS Appl. Mater. Interfaces 2015, 7, 6293−6299

of human leukemic K562 line.[16−18] The grafting method, which relied on conjugating APTES to the surface of the thermoplastics treated by oxygen plasma, was an extension of a method developed by Sunkara et al. to covalently graft APTES to various thermoplastics including polycarbonate, cyclic olefin copolymer, poly(methyl methacrylate), and polystyrene.[21] We applied this method to PLGA in this study. To covalently graft PAH to the APTES-coated PLGA, we used glutaraldehyde as a cross-linker. To examine the outcomes of the key grafting steps, we used FITC, which bonds to primary amine and fluoresces, as an indicator. The results in Figure 2 suggested successful conjugation of APTES to PLGA and PAH to APTES, respectively, as expected. The above surface-grafting method was combined with μCP to produce microdevices as shown in Figure 3. The printed microdevices were highly uniform in size, shape, and fluorescence intensity. The thickness determined by AFM measurement allowed the characterization of drug-loading capacity and efficiency for the microdevices.

In an envisaged therapy using our microdevices, the microdevices will first be bulk-mixed with live therapeutic cells to form the cell−microdevice complexes without aggregated cells, and the complexes will be administered into the bloodstream of the patients. To prove that the necessity of the asymmetric structure shown in Figure 1, we fabricated two types of symmetric microdevices with the same shape and lateral diameter as the asymmetric microdevices. One was composed of plain PLGA. The other was made of a polyelectrolyte multilayer with PAH being the outermost layer materials for both faces. The PLGA microdevices were expected not to bind to the cells, and the polyelectrolyte multilayered microdevices were expected to cross-link cells. The result (Figure 4A,B) was consistent with the expectation. In contrast, our asymmetric microdevices bound to the cells without cross-linking the cells (Figure 4C). The results clearly proved that the asymmetric structure was essential for the intended application. Compared to results reported in ref 15, absence of cell aggregation here might be attributable to the use of the covalent bonding for constructing the microdevices rather than the noncovalent interactions. The mixture of the asymmetric microdevices and the cells was further characterized with flow cytometry (Figure 4D). While this measurement allowed a quick counting of large numbers of free cells, free microdevices, and cell−microdevice complexes, it could not differentiate complexes carrying different numbers of microdevices per cell. A manual counting using a homemade hemocytometer was thus performed. The result (Figure 4E) indicates that majority of the complexes prepared at a microdevice-to-cell ratio of 1:1 consisted of one cell and one microdevice. Moreover, the similarity between the experimental result and the simulations and calculation at different maximum numbers of microdevices per cell suggests that the cells possessed a uniform capacity to bind to the microdevices. Moreover, the insensitivity of the cell distribution to the maximum numbers of microdevices per cell indicates that a similar distribution is expected when nanometer-sized devices were used.[4]

The number of the microdevices in each complex is obviously important in affecting the performance of this drug delivery system through influencing the drug-loading capacity of the cells and the interactions between the complexes and the in vivo environments. An advantage of bulk mixing is to allow easy manipulation of the number of the microdevices in the complexes by controlling the microdevice-to-cell ratio. The feasibility was demonstrated in Figure 4F, which clearly showed that the complexes prepared at microdevice-to-cell ratio of 3:1 contained more microdevices on average than those in Figure 4C. With respect to composition of the microdevices, both the drug-laden thermoplastic and cell-adhesive polyelectrolyte are important in determining the functionalities of the microdevices. In addition to PLGA, two other biocompatible and biodegradable thermoplastics, namely, PLA and PCL, which have different degradation and drug loading and releasing properties from PLGA, were used here to demonstrate the potential of the microdevices for versatile drug-delivery applications (Figure 4F). Besides PAH, two other polyelectrolytes—PLL and PEI—were used as the cell-adhesive polyelectrolytes. Note that PLL as a polypeptide is intrinsically biodegradable. Moreover, many other commonly used cell-adhesive substances such as antibodies can, in principle, be covalently conjugated to the APTES-coated surface to allow forming the complexes through a specific interaction such as the IgG-Fc receptor interaction as demonstrated by Anselmo et al.[13] In addition, we demonstrated attaching different microdevices to a single cell (Figure 4F), indicating that this method can be used to prepare complexes carrying multiple drugs and even other functional materials.

The intended application of the cell-borne microdevices probably requires that the cell in a cell−microdevice complex is not killed or severely injured by the microdevice. We therefore studied viability of K562 cells mixed with the PLGA/APTES/glutaraldehyde/PAH microdevices. The result (Figure 5A) shows that concentration of live cells remained almost the same as that of live cells not mixed with the microdevices, indicating that presence of the microdevices did not influence the overall viability of the cells. However, this observation did not exclude the possibility that division of the bound cells was significantly inhibited, but the unbound cells divided at an increased rate. To assess this possibility, cells of half starting concentration without being mixed with the microdevices were cultured under the same condition. Its growth curve was significantly different from the other two curves. It is thus clear that the cells bound by the microdevices were viable and proliferated. We also counted cell−microdevice complexes and all microdevices (including both bound and free ones) at different time points. As show in Figure 5B, the concentration of all microdevices remained largely constant over 7 d, indicating that the microdevices did not degrade during this period of time. However, the concentration of the cell−microdevice complexes decreased gradually slightly. At day 7, ∼60 wt % of the original complexes remained, indicating the complexes were largely stable over this period of time.

Acridine orange was used as a mock drug in this study due to its strong fluorescence, which allowed sensitive and convenient measurement of its concentration in a solution. Its successful loading into the microdevices and subsequent release as shown in Figure 6 proves the feasibility of loading a real drug into our asymmetric microdevices and achieving sustained release of the drug from the microdevices. Note that PLGA, PLA, and PCL were used to prepare micro/nanoparticles for the delivery of a wide range of therapeutics ranging from small-molecule drugs to macromolecular biologicals such as proteins.[22] For example, DeSimone's group fabricated docetaxel-laden PLGA nanoparticles with a loading capacity of 40 wt % using a soft lithographic method.[23]

The ultimate goal of this research is to develop a clinically useful cell-borne drug-delivery system. Our microdevices are particularly suitable for sustained intravascular drug delivery when RBCs are used as the carriers for the following reasons. First, the covalent bonds used for constructing the microdevices

DOI: 10.1021/acsami.5b00613
ACS Appl. Mater. Interfaces 2015, 7, 6293−6299

would maximize the structural stability of the microdevices in vivo over a relatively long period of time. Second, the viability and functionalities of the cells bound by the microdevices probably would not be affected. Third, drugs can likely be released from the microdevices over the same period of time. It is also important to note that our method for fabricating the microdevices is inexpensive and can potentially be scaled up for large-scale manufacturing.[24]

5. CONCLUSIONS

We have developed a novel soft lithographic method for fabricating microdevices for cell-borne drug delivery. The microdevices feature a disklike shape, an asymmetric structure, the use of biodegradable thermoplastics as the major component material, and the use of covalent bonds to hold the component materials together. We have found that the microdevices could bind to live cells through bulk mixing without causing cell aggregation. The binding was largely stable and did not affect the viability and proliferation ability of the cells over at least a week. Moreover, we have demonstrated loading a mock drug into the microdevices and sustained release of the mock drug from the microdevices. The microdevices hold potential to be further developed into a clinically useful cell-borne drug-delivery system.

■ ASSOCIATED CONTENT

Supporting Information

Standard curves of concentration of acridine orange in PBS and ethanol. This material is available free of charge via the Internet at http://pubs.acs.org.

■ AUTHOR INFORMATION

Corresponding Author

*Phone: 18504106643. Fax: 18504106150. E-mail address: guan@eng.fsu.edu.

Notes

The authors declare no competing financial interest.

■ ACKNOWLEDGMENTS

The authors thank Ms. R. Didier of Department of Biomedical Sciences, College of Medicine, Florida State University (FSU), for her help on flow cytometry. This study was supported by FSU Startup Funds and National Science Foundation Award No. 1300447.

■ REFERENCES

(1) Chambers, E.; Mitragotri, S. Prolonged Circulation of Large Polymeric Nanoparticles by Non-covalent Adsorption on Erythrocytes. *J. Controlled Release* **2004**, *100*, 111−119.

(2) Chambers, E.; Mitragotri, S. Long Circulating Nanoparticles via Adhesion on Red Blood Cells: Mechanism and Extended Circulation. *Exp. Biol. Med. (London, U. K.)* **2007**, *232*, 958−966.

(3) Cheng, H.; Kastrup, C. J.; Ramanathan, R.; Siegwart, D. J.; Ma, M.; Bogatyrev, S. R.; Xu, Q.; Whitehead, K. A.; Langer, R.; Anderson, D. G. Nanoparticulate Cellular Patches for Cell-Mediated Tumoritropic Delivery. *ACS Nano* **2010**, *4*, 625−631.

(4) Stephan, M. T.; Moon, J. J.; Um, S. H.; Bershteyn, A.; Irvine, D. J. Therapeutic Cell Engineering with Surface-conjugated Synthetic Nanoparticles. *Nat. Med. (N. Y., NY, U. S.)* **2010**, *16*, 1035−1041.

(5) Tao, S. L.; Lubeley, M. W.; Desai, T. A. Bioadhesive Poly(methyl methacrylate) Microdevices for Controlled Drug Delivery. *J. Controlled Release* **2003**, *88*, 215−228.

(6) Cohen, M. H.; Melnik, K.; Boiarski, A. A.; Ferrari, M.; Martin, F. J. Microfabrication of Silicon-based Nanoporous Particulates for Medical Applications. *Biomed. Microdevices* **2003**, *5*, 253−259.

(7) Rolland, J. P.; Maynor, B. W.; Euliss, L. E.; Exner, A. E.; Denison, G. M.; DeSimone, J. M. Direct Fabrication and Harvesting of Monodisperse, Shape-specific Nanobiomaterials. *J. Am. Chem. Soc.* **2005**, *127*, 10096−10100.

(8) Guan, J.; He, H.; Lee, L. J.; Hansford, D. J. Fabrication of Particulate Reservoir-containing, Capsulelike, and Self-folding Polymer Microstructures for Drug Delivery. *Small* **2007**, *3*, 412−418.

(9) Ainslie, K. M.; Kraning, C. M.; Desai, T. A. Microfabrication of an Asymmetric, Multi-layered Microdevice for Controlled Release of Orally Delivered Therapeutics. *Lab Chip* **2008**, *8*, 1042−1047.

(10) Chirra, H. D.; Shao, L.; Ciaccio, N.; Fox, C. B.; Wade, J. M.; Ma, A.; Desai, T. A. Planar Microdevices for Enhanced in vivo Retention and Oral Bioavailability of Poorly Permeable Drugs. *Adv. Healthcare Mater.* **2014**, *3*, 1648−1654.

(11) Guan, J.; Ferrell, N.; Lee, L. J.; Hansford, D. J. Fabrication of Polymeric Microparticles for Drug Delivery by Soft Lithography. *Biomaterials* **2006**, *27*, 4034−4041.

(12) Swiston, A. J.; Cheng, C.; Um, S. H.; Irvine, D. J.; Cohen, R. E.; Rubner, M. F. Surface Functionalization of Living Cells with Multilayer Patches. *Nano Lett.* **2008**, *8*, 4446−4453.

(13) Anselmo, A. C.; Gilbert, J. B.; Kumar, S.; Gupta, V.; Cohen, R. E.; Rubner, M. F.; Mitragotri, S. Monocyte-mediated Delivery of Polymeric Backpacks to Inflamed Tissues: A Generalized Strategy to Deliver Drugs to Treat Inflammation. *J. Controlled Release* **2015**, *199*, 29−36.

(14) Doshi, N.; Swiston, A. J.; Gilbert, J. B.; Alcaraz, M. L.; Cohen, R. E.; Rubner, M. F.; Mitragotri, S. Cell-based Drug Delivery Devices Using Phagocytosis-resistant Backpacks. *Adv. Mater. (Weinheim, Ger.)* **2011**, *23*, H105−H109.

(15) Swiston, A. J.; Gilbert, J. B.; Irvine, D. J.; Cohen, R. E.; Rubner, M. F. Freely Suspended Cellular "Backpacks" Lead to Cell Aggregate Self-assembly. *Biomacromolecules* **2010**, *11*, 1826−1832.

(16) Zhang, P.; Guan, J. Fabrication of Multilayered Microparticles by Integrating Layer-by-layer Assembly and Microcontact Printing. *Small* **2011**, *7*, 2998−3004.

(17) Zhang, P.; Liu, Y.; Xia, J.; Wang, Z.; Kirkland, B.; Guan, J. Top-down Fabrication of Polyelectrolyte-thermoplastic Hybrid Microparticles for Unidirectional Drug Delivery to Single Cells. *Adv. Healthcare Mater.* **2013**, *2*, 540−545.

(18) Wang, Z.; Xia, J.; Yan, Y.; Tsai, A. C.; Li, Y.; Ma, T.; Guan, J. Facile Functionalization and Assembly of Live Cells with Microcontact Printed Polymeric Biomaterials. *Acta Biomater.* **2015**, *11*, 80−87.

(19) Morton, S. W.; Herlihy, K. P.; Shopsowitz, K. E.; Deng, Z. J.; Chu, K. S.; Bowerman, C. J.; DeSimone, J. M.; Hammond, P. T. Scalable Manufacture of Built-to-Order Nanomedicine: Spray-assisted Layer-by-layer Functionalization of PRINT Nanoparticles. *Adv. Mater. (Weinheim, Ger.)* **2013**, *25*, 4707−4713.

(20) Johnson, N. L.; Kotz, S. *Urn Models and Their Application: An Approach to Modern Discrete Probability Theory;* John Wiley & Sons Inc: New York, 1977; Chapter 3, p 114.

(21) Sunkara, V.; Park, D. K.; Hwang, H.; Chantiwas, R.; Soper, S. A.; Cho, Y. K. Simple Room Temperature Bonding of Thermoplastics and Poly(dimethylsiloxane). *Lab Chip* **2011**, *11*, 962−965.

(22) Kumari, A.; Yadav, S. K.; Yadav, S. C. Biodegradable Polymeric Nanoparticles Based Drug Delivery Systems. *Colloids Surf., B* **2010**, *75*, 1−18.

(23) Enlow, E. M.; Luft, J. C.; Napier, M. E.; DeSimone, J. M. Potent Engineered PLGA Nanoparticles by Virtue of Exceptionally High Chemotherapeutic Loadings. *Nano Lett.* **2011**, *11*, 808−813.

(24) Xia, Y.; Qin, D.; Whitesides, G. M. Microcontact Printing with A Cylindrical Rolling Stamp: A Practical Step toward Automatic Manufacturing of Patterns with Submicrometer-sized Features. *Adv. Mater. (Weinheim, Ger.)* **1996**, *8*, 1015−1017.

DOI: 10.1021/acsami.5b00613
ACS Appl. Mater. Interfaces 2015, 7, 6293−6299